

SUPPORTING INFORMATION

Copper complexes with tetradentate ligands for enhanced charge transport in Dye-Sensitized Solar Cells

Hannes Michaels, Iacopo Benesperi, Tomas Edvinsson, Ana Belen Muñoz-García, Michele Pavone, Gerrit Boschloo, Marina Freitag

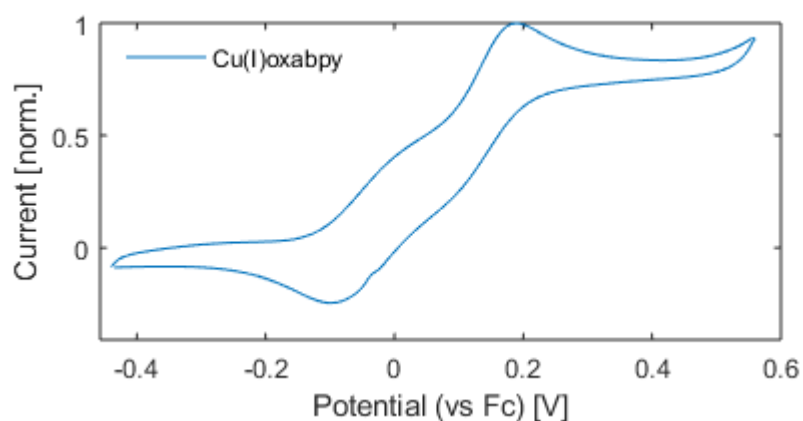


Figure S1: Cyclic voltammogram of 5 mM Cu^I(oxabpy) in acetonitrile (0.1 M TBAPPF₆). The calibration of the Ag/AgCl reference electrode against the ferrocene/ferrocenium redox couple (0.62 V vs NHE) yielded a formal potential of 0.66 V vs NHE for the Cu(oxabpy) redox system.

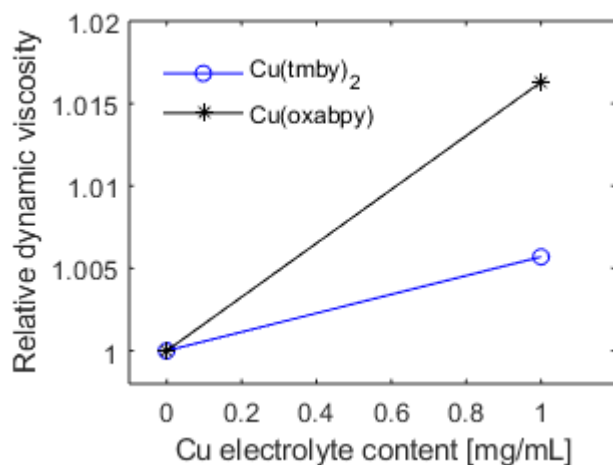


Figure S2: Relative dynamic viscosity of chloroform upon addition of 10 mg/mL Cu^{III}(tmby)₂ (blue) and Cu^{III}(oxabpy) complexes (black). Within the 10 mg/mL, the complexes were added in the molar ratio of the best-performing solar cells (Cu^I 5:1 Cu^{II}).

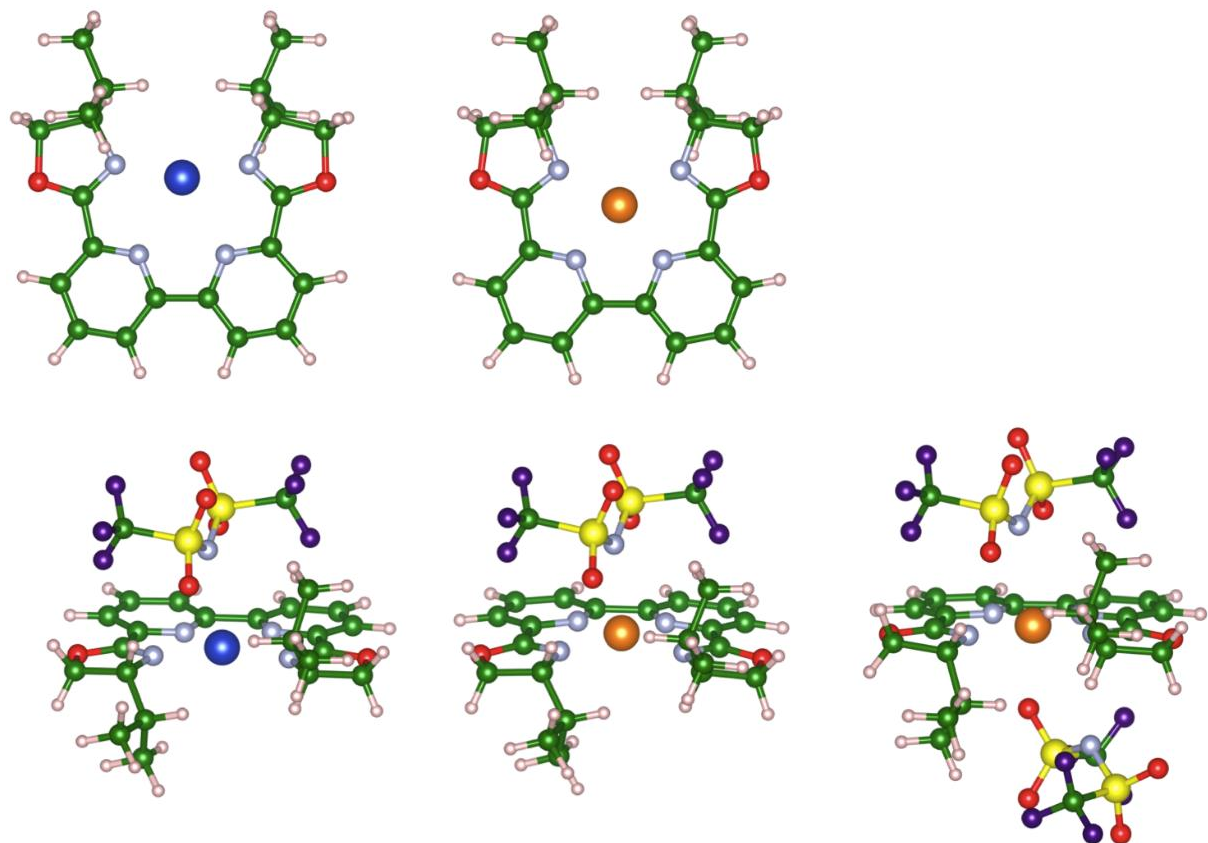


Figure S3: Lowest-energy structures for $\text{Cu}^{\text{I}}(\text{oxabpy})$ (left, blue metal center) and $\text{Cu}^{\text{II}}(\text{oxabpy})$ (right, orange metal center). Bottom row: $\text{Cu}^{\text{I}}(\text{oxabpy})$ with TFSI counterion and $\text{Cu}^{\text{II}}(\text{oxabpy})$ with one and two TFSI counterions, respectively.

Table S1 : Vertical excitation energies (λ in nm) and corresponding oscillator strengths (f) for the $\text{Cu}^{\text{II}}(\text{oxabpy})$ complexes in acetonitrile solution computed with TD-DFT. We also considered the minimum-energy structures of the $\text{Cu}^{\text{I}}/\text{Cu}^{\text{II}}(\text{oxabpy})$ complexes with 1 TFSI molecule attached to the Cu cation.

	wavelength [nm]	f
$\text{Cu}^{\text{I}}(\text{oxabpy})$	486	0.0009
	391	0.0232
$\text{Cu}^{\text{I}}(\text{oxabpy})\text{-TFSI}$	524	0.0014
	417	0.0231
$\text{Cu}^{\text{II}}(\text{oxabpy})$	560	0.0007
$\text{Cu}^{\text{II}}(\text{oxabpy})\text{-TFSI}$	670	0.0001

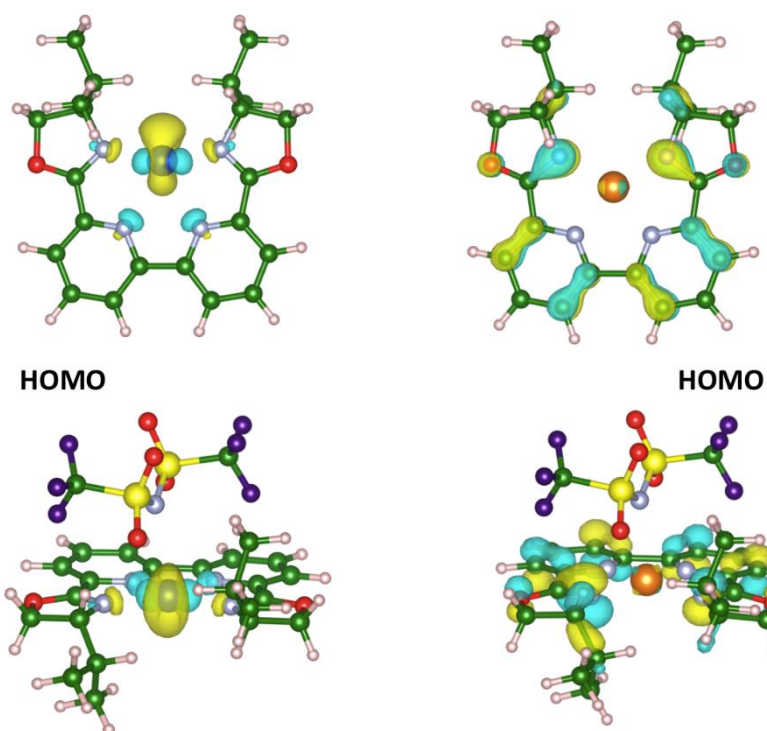


Figure S4: Highest-occupied molecular orbitals (HOMO) for $\text{Cu}^{\text{I}}(\text{oxabpy})$ (left) and $\text{Cu}^{\text{II}}(\text{oxabpy})$ (right). No significant change in frontier orbitals is observed upon coordination of a TFSI counterion.

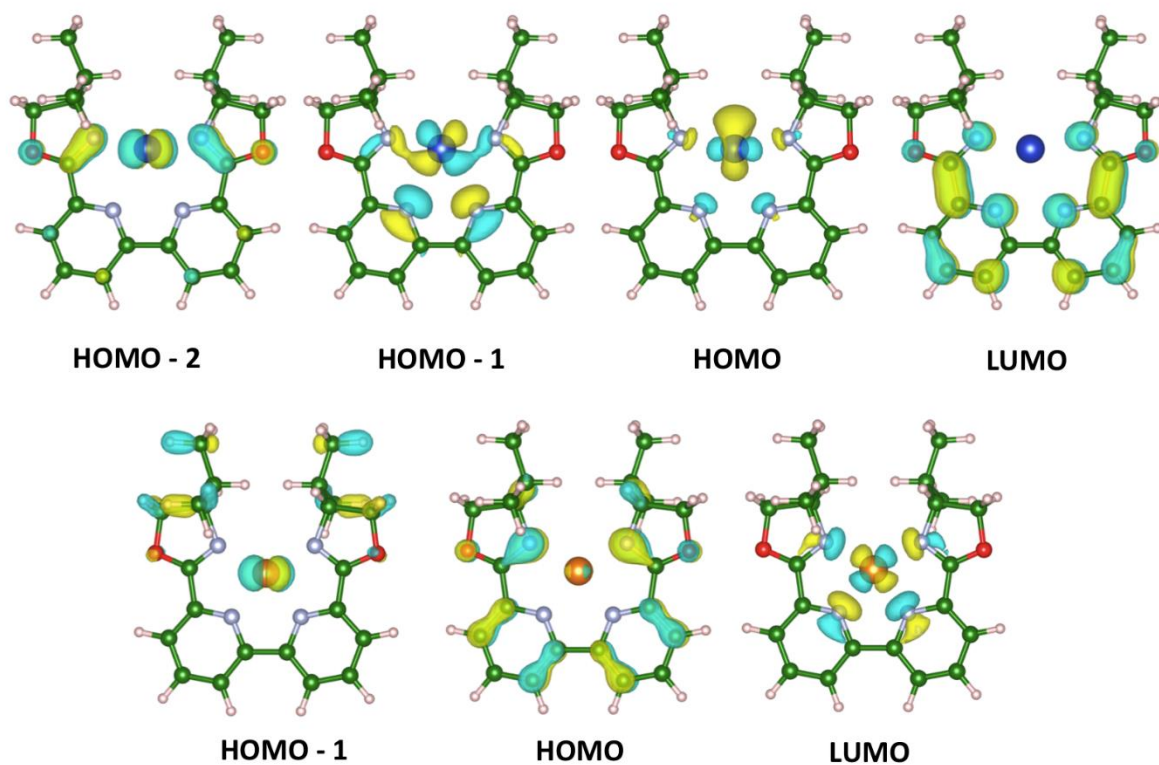


Figure S5: Isodensity (0.05) surfaces for frontier orbitals in $\text{Cu}^{\text{I}}(\text{oxabpy})$ (top) and $\text{Cu}^{\text{II}}(\text{oxabpy})$ (bottom).

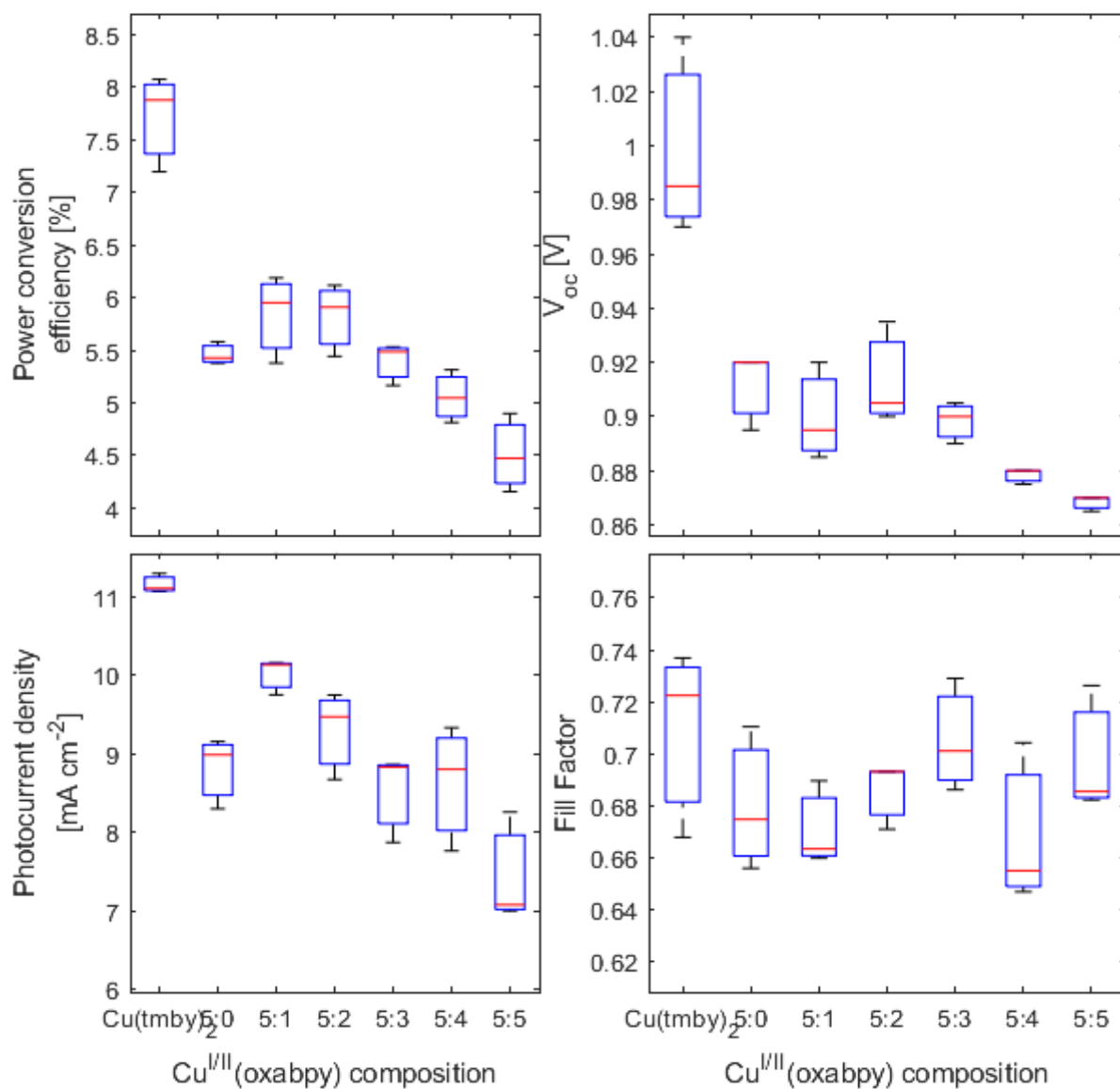


Figure S6: Parameters of the photovoltaic performance for the $\text{Cu}(\text{tmby})_2$ reference electrolyte (left) and $\text{Cu}(\text{oxabpy})$ with respect to the addition of $\text{Cu}^{\text{II}}(\text{oxabpy})$ to the electrolyte (5:0 = Cu^{I} only, 5:1 = standard electrolyte 0.2 M Cu^{I} , 0.04 M Cu^{II})

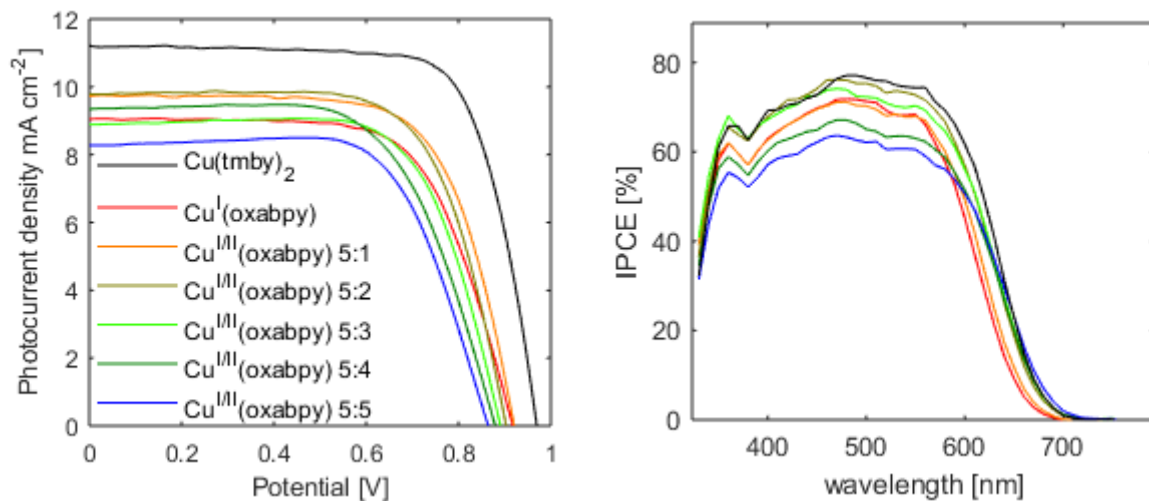


Figure S7: Photovoltaic performance. (a) Current density vs applied potential and (b) incident photon-to-current conversion efficiency for Y123-sensitized DSCs. The color code indicates the ratio of Cu^{II} in the $\text{Cu}(\text{oxabpy})$ electrolyte (orange = standard electrolyte 0.2 M Cu^{I} , 0.04 M Cu^{II} ; (blue) = 1:1 mixture).

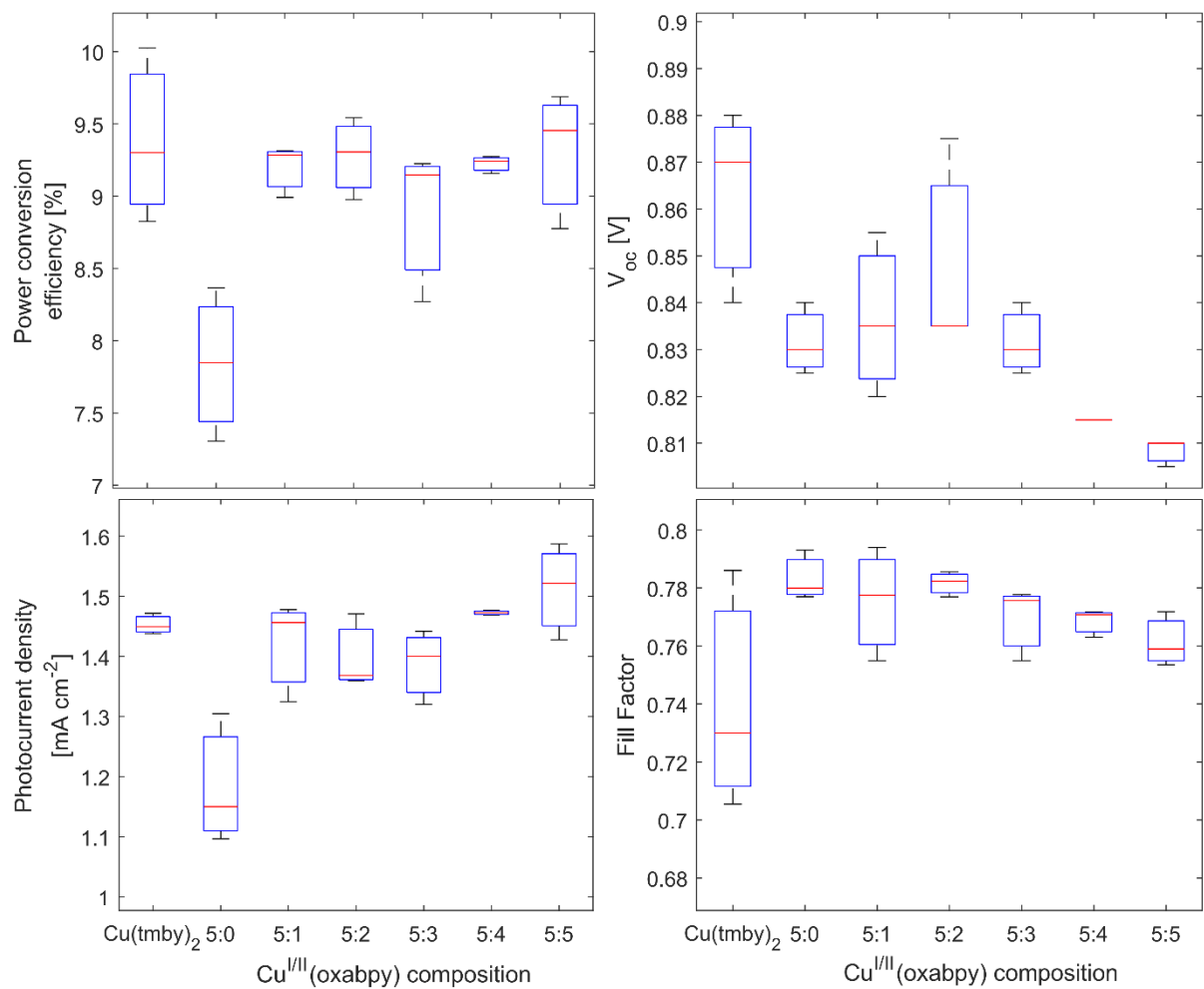


Figure S8: Parameters of the photovoltaic performance at 10 mW cm^{-2} light intensity for the $\text{Cu}(\text{tmby})_2$ reference electrolyte (left) and $\text{Cu}(\text{oxaby})$ with respect to the addition of $\text{Cu}^{\text{II}}(\text{oxaby})$ to the electrolyte (5:0 = Cu^{I} only, 5:1 = standard electrolyte $0.2 \text{ M Cu}^{\text{I}}$, $0.04 \text{ M Cu}^{\text{II}}$).

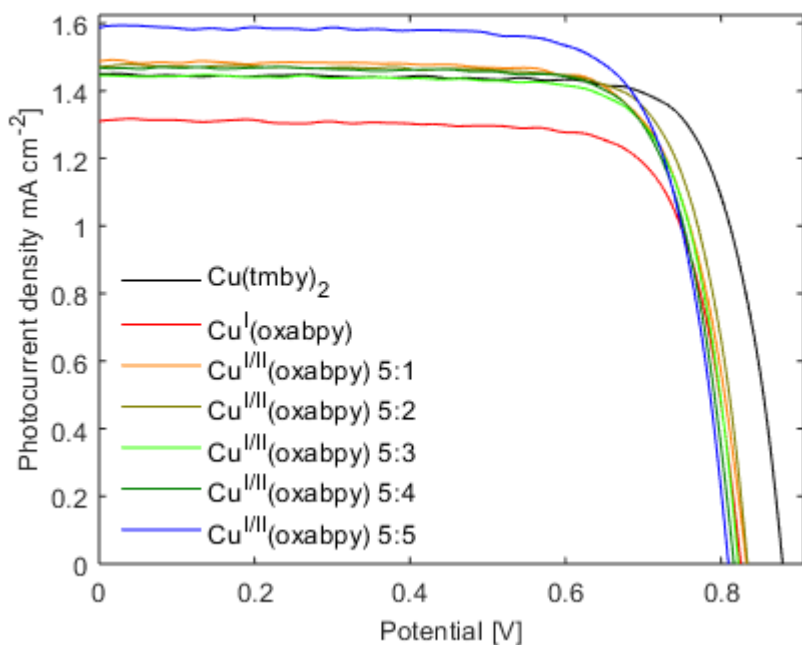


Figure S9: Photovoltaic performance at 10 mW cm^{-2} illumination. Current density vs applied potential for Y123-sensitized DSCs. The color code indicates the ratio of Cu^{II} in the $\text{Cu}(\text{oxabpy})$ electrolyte (orange = standard electrolyte $0.2 \text{ M Cu}^{\text{I}}$, $0.04 \text{ M Cu}^{\text{II}}$; (blue) = 1:1 mixture).

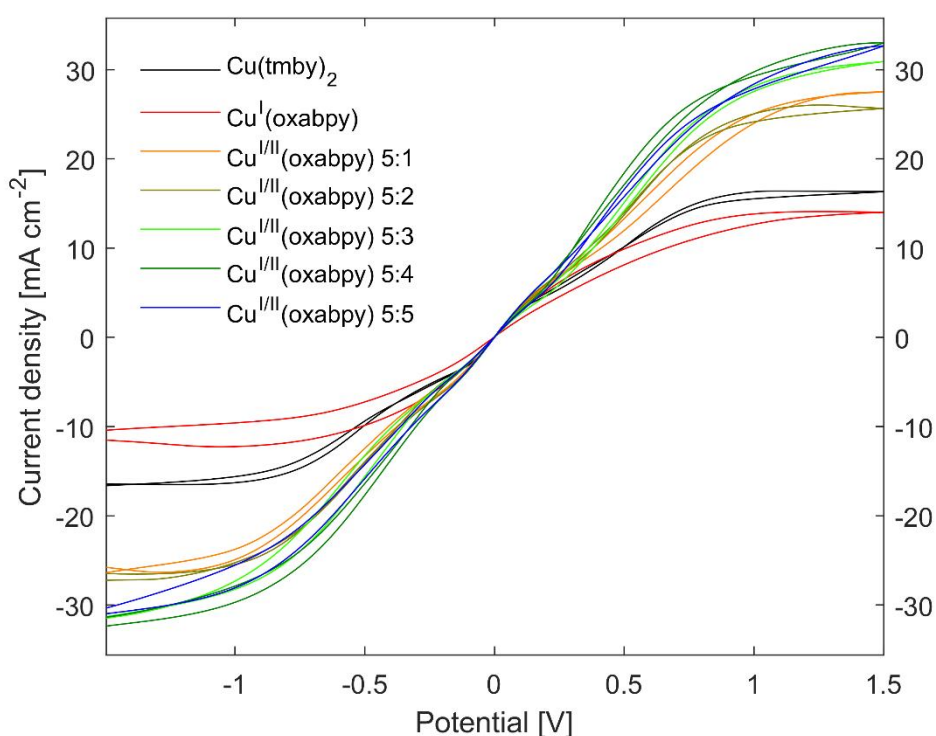


Figure S10: Electrochemical characterization of symmetrical PEDOT-PEDOT cells with cyclic voltammetry (25 mV/s). The color code indicates the ratio of Cu^{II} in the $\text{Cu}(\text{oxabpy})$ electrolyte (orange = standard electrolyte $0.2 \text{ M Cu}^{\text{I}}$, $0.04 \text{ M Cu}^{\text{II}}$; (blue) = 1:1 mixture).

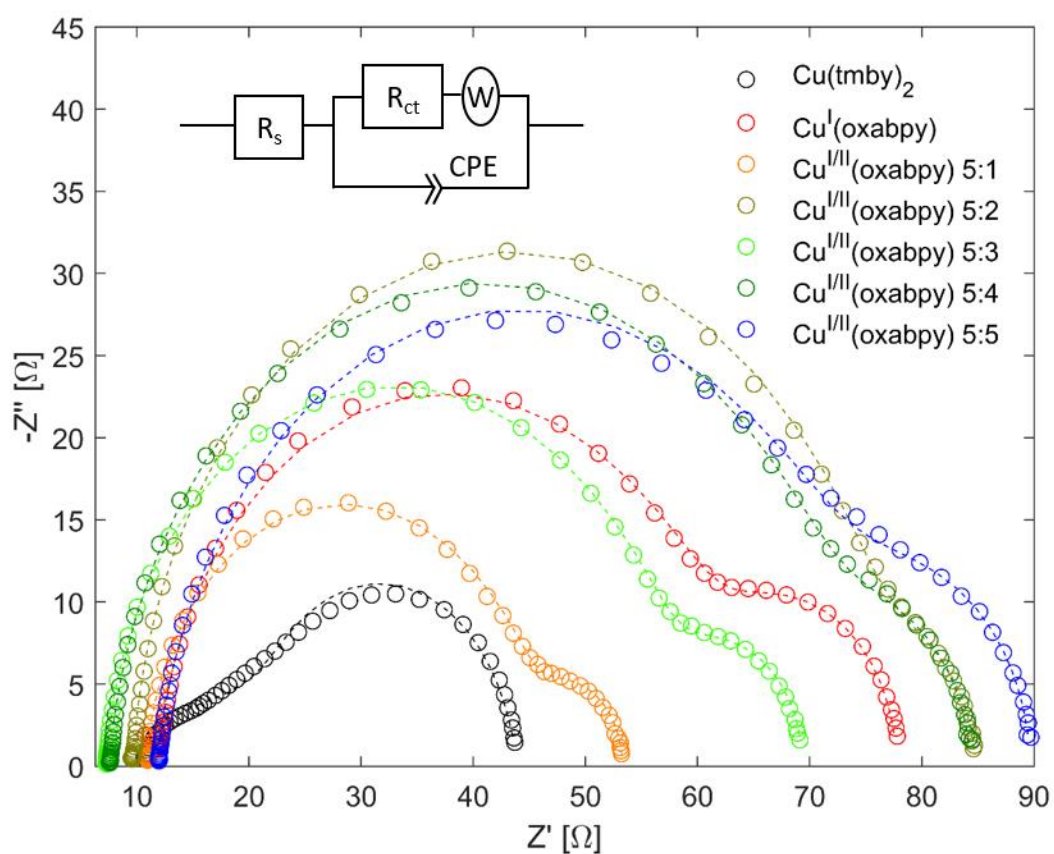


Figure S11: Electrochemical impedance spectra of symmetrical PEDOT-PEDOT cell recorded at zero-potential; the circles indicate experimentally collected data points, dashed lines represent fits to the alternative circuit model (inlet). The color code indicates the ratio of Cu^{II} in the $Cu(oxabpy)$ electrolyte (orange = standard electrolyte 0.2 M Cu^I , 0.04 M Cu^{II} ; (blue) = 1:1 mixture).

Table S2: Electrochemical characterization of PEDOT-PEDOT cells. The first two rows list current density J_L and diffusion coefficient D from the cyclovoltammograms. The equivalent circuit parameters for the electrochemical impedance spectra are: serial resistance R_s , charge transfer resistance R_{CT} , frequency-independent parameters Q and β for the constant phase element and resistance R_w as well as time constant T_w for the Warburg diffusion model. Diffusion coefficients from the electrochemical impedance spectra are shown in the last row. The diffusion coefficients were calculated from equations (2) and (5), respectively. Previously reported values in parenthesis.

	Cu(tmby) ₂	Cu ^I (oxabpy)	Cu ^{II} (oxabpy)				
			5:1	5:2	5:3	5:4	5:5
J_L [mA cm ⁻²]	16.6	14.1	27.5	26.0	30.9	33.0	32.7
D [10 ⁻⁶ cm ² s ⁻¹] for Cu ^{II} from J_L	8.6		14.3				
R_s [Ω]	10.5	11.8	10.8	9.23	7.21	7.57	8.42
R_{CT} [Ω]	6.92	48.5	33.4	30.6	50.1	64.1	38.6
CPE: Q [10 ⁻³ Ω ⁻¹ s ^{-β}]	0.337	0.156	0.124	0.145	0.154	0.137	0.169
CPE: β	0.847	0.936	0.967	0.945	0.931	0.930	0.892
W: R_w [Ω]	26.5	17.3	9.09	12.2	11.9	12.9	22.0
W: T_w [s]	0.208	0.374	0.285	0.540	0.451	0.293	0.414
D [10 ⁻⁶ cm ² s ⁻¹] for Cu ^{II} from R_w	22.4		63.7				